



PII S0038-1098(96)00295-5

STRUCTURE AND MAGNETIC PROPERTIES OF THE PYROCHLORE $\text{Sc}_2\text{Mn}_2\text{O}_7$

J. E. Greedan,* N. P. Raju * and M. A. Subramanian †

* Brockhouse Institute for Materials Research, McMaster University, Hamilton, Ontario L8S 4M1, Canada

† E.I. du Pont de Nemours and Co., Experimental Station, Wilmington, DE 19898, U.S.A.

(Received 10 April 1996; accepted 26 April 1996 by M. Collins)

$\text{Sc}_2\text{Mn}_2\text{O}_7$ has been prepared at 60 kbar and the crystal structure has been determined from Rietveld analysis of x-ray powder diffraction data. A cubic pyrochlore structure is found described in space group $\text{Fd}\bar{3}\text{m}$ with $a=9.5965(4)$ Å. Magnetic susceptibility data conform to the Curie-Weiss law in the range 175 K to 300 K with an effective moment of $3.6(1) \mu_{\text{B}}/\text{Mn}$ and $\theta_p = +77(3)$ K indicating the predominance of ferromagnetic interactions. Nonetheless, the material does not show long range magnetic order and instead a spin glass like transition is found below 17 K. Thus, $\text{Sc}_2\text{Mn}_2\text{O}_7$ resembles $\text{Y}_2\text{Mn}_2\text{O}_7$ and $\text{Lu}_2\text{Mn}_2\text{O}_7$, both spin glass materials, rather than $\text{In}_2\text{Mn}_2\text{O}_7$ and $\text{Tl}_2\text{Mn}_2\text{O}_7$ which are ferromagnetic below 120 K. The compound is red-orange in color and is an insulator in contrast to the other manganese pyrochlores which are semiconductors.

Copyright © 1996 Elsevier Science Ltd

Keywords: A. Spin glasses, A. magnetically ordered materials, C. Crystal structure and symmetry.

1. Introduction

PYROCHLORE STRUCTURE oxides of composition $\text{R}_2\text{Mn}_2\text{O}_7$ have been the subject of recent investigations [1-8]. In order to stabilize the Mn(IV) oxidation state, high pressure methods are necessary. For the cases where R is a rare earth, $\text{R} = \text{Dy-Lu}$ and Y, hydrothermal methods and 3 kbar pressure are adequate but for $\text{R} = \text{In, Tl}$ or Sc much higher pressures of the order of 60 kbar are requisite [1-3]. Structural studies using either single crystal x-ray or powder neutron diffraction data indicate a well-ordered pyrochlore structure, space group $\text{Fd}\bar{3}\text{m}$ with R in 16d, Mn in 16c, O1 in 48f and O2 in 8b [3,6,8]. There is little evidence for mixing of R and Mn on the two cation sites or for oxygen vacancies beyond the 1-2% level which is essentially the detection limit for diffraction methods.

Physical characterization to date has consisted of fairly extensive magnetic, neutron scattering and specific heat studies of selected compounds and a complex picture has emerged [4-6]. From analysis of magnetic susceptibility data all of the materials appear to be ferromagnetic as values of the θ_p range from +40 K to +155 K. Yet, when examined more closely, behavior consistent with a spin glass like state is found at low temperatures, 7 K - 35 K, for the cases where R is a lanthanide or Y [4,6]. Contrastingly, for $\text{R} = \text{In}$ or Tl there is evidence for true

long range ferromagnetic order at 120 K from magnetic studies and small angle neutron scattering although corroboration from specific heat and neutron diffraction is lacking [5].

Information from transport measurements is yet very sparse but the $\text{R} = \text{lanthanide}$ series members are semiconductors with room temperature resistivities between 10^6 and $10^8 \Omega\text{-cm}$ and activation energies in the range of 0.4 to 0.5 eV [3]. Room temperature resistivities for $\text{R} = \text{In}$ and Tl are significantly lower, $10^4 \Omega\text{-cm}$ for In and $10 - 10^1 \Omega\text{-cm}$ for Tl depending on the sample studied [4]. For $\text{R} = \text{Tl}$ there is a strong coupling between magnetic and transport properties in the form of a sharp decrease by factors of $10 - 10^2$ in the resistivity near T_c [4]. Not surprisingly, so-called giant magneto-resistance (GMR) has been reported for this material recently [7]. $\text{Sc}_2\text{Mn}_2\text{O}_7$ has not been studied in detail although a brief report on the low temperature magnetization exists [2].

2. Experimental

(a) Synthesis of $\text{Sc}_2\text{Mn}_2\text{O}_7$

Stoichiometric quantities of Sc_2O_3 (99.99%, Aldrich) and MnO_2 (Specpure, Johnson and Matthey) were mixed thoroughly together in an agate mortar. About 300 mg of the mixture was sealed into a gold capsule and heated to

850 °C for 1 hour at 60 kbar pressure in a tetrahedral anvil. The capsule was cooled rapidly to room temperature before releasing the pressure and a reddish orange product was isolated.

(b) X-ray Diffraction

Powder diffraction data were collected both with a Guinier-Hägg camera (IRDAB XDC700) using $\text{Cu K}\alpha_1$ radiation and a Si internal standard, and a diffractometer (Nicolet I2) with $\text{Cu K}\alpha$ radiation and a graphite monochromator on the exit beam. The Guinier films were read with a computer-controlled line scanner (KEJ Instruments, Täby, Sweden). Rietveld refinement was carried out on a 80486 PC using the program package DBWS-9006PC, a 1991 release of DBWS3.2S by Wiles and Young [9].

(c) Magnetic Measurements

Magnetic susceptibility data were obtained using a Quantum Design SQUID magnetometer in the range 5 to 300 K at an applied field of 0.005T (50 Oe). Isothermal magnetization data were collected at 5 K for fields up to 5.5 T.

3. Results and Discussion

(a) Structural Aspects

The powder diffraction pattern for $\text{Sc}_2\text{Mn}_2\text{O}_7$ is shown in Fig. 1. All peaks can be assigned to a cubic pyrochlore cell except for one very weak feature at about $2\theta = 52.5^\circ$ which is assigned to Sc_2O_3 and thus, a two phase Rietveld

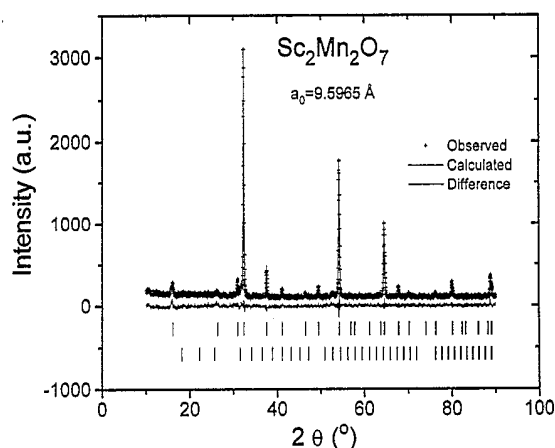


Fig. 1: X-ray powder diffraction data for $\text{Sc}_2\text{Mn}_2\text{O}_7$ at room temperature. Solid line through the data points shows the profile obtained by Rietveld analysis. Lower solid line corresponds to the difference between the fit and the data. Upper and lower vertical bars indicate the possible reflections for $\text{Sc}_2\text{Mn}_2\text{O}_7$ and Sc_2O_3 phases, respectively.

refinement was attempted [10]. The fit is excellent and the details are given in Tables I and II. Selected values of the derived bond distances and angles are displayed in Table III. The Sc_2O_3 content was determined to be 2.3(2) wt%.

Table I. X-ray powder profile refinement results for $\text{Sc}_2\text{Mn}_2\text{O}_7$. Two phase refinement.

Space group	Fd3m (No. 2)
a_0 (Å)	9.5965(4)
Lineshape	Pseudo-Voigt
Setp width (2θ)	0.03°
R_p	0.0753
R_{wp}	0.0970
R_E	0.0821
S^a	1.18
D- W^b	1.03
No. parameters	17
Observed data	2685
Independent hkl	25
2θ range	10° - 90°
Temperature	293 K
Scale factor ($\text{Sc}_2\text{Mn}_2\text{O}_7$)	$3.71(4) \times 10^{-5}$
Scale factor (Sc_2O_3)	$9.2(9) \times 10^{-7}$

$$R_p = \frac{\sum |Y_{OBS} - Y_{CAL}/c|}{\sum |Y_{OBS}|}, \quad R_{wp} = \left[\frac{\sum w(Y_{OBS} - Y_{CAL}/c)^2}{\sum wY_{OBS}^2} \right]^{1/2}, \quad R_E = \left[\frac{(N-P)}{\sum wY_{OBS}^2} \right]^{1/2}$$

^a Square root of goodness-of-fit, ^b Weighted Durbin-Watson statistic

Table II. Refined atomic coordinates and thermal parameters for $\text{Sc}_2\text{Mn}_2\text{O}_7$.

Atom	Position	x	y	z	B (Å ²)
Sc	16d	0.5	0.5	0.5	1.99(12)
Mn	16c	0.0	0.0	0.0	1.56(10)
O1	8b	0.375	0.375	0.375	0.82(62)
O2	48f	0.125	0.125	0.3342(7)	1.34(19)

The unit cell constant found from the Rietveld analysis is larger than that reported previously, 9.586 Å, but in reasonable agreement with the value determined from the Guinier data of $a = 9.592(1)$ Å [2]. Note, Table III, that the Mn-O distance, 1.879(3) Å is significantly shorter than the values of 1.90 - 1.91 Å reported for the other $\text{R}_2\text{Mn}_2\text{O}_7$ pyrochlores. This shortened bond length is most likely due to the chemical pressure provided by the small Sc^{3+} ion and not to any mixed valence on the Mn site as the material is red-orange in color and not black as for most mixed valence systems involving Mn. The shorter bond

Table III. Selected bond distances (Å) and angles (°) for $\text{Sc}_2\text{Mn}_2\text{O}_7$.

Sc - O1 (×2)	2.0777(1)
Sc - O2 (×6)	2.326(5)
Mn - O2 (×6)	1.879(3)
O2 - Mn - O2	180
O2 - Mn - O2	98.1(1)
O2 - Mn - O2	81.9(1)
Mn - O2 - Mn	129.1(4)
O1 - Sc - O1	180
O1 - Sc - O2	101.6(1)
O1 - Sc - O2	78.43(8)
O2 - Sc - O2	63.9(1)
O2 - Sc - O2	116.1(1)

length may have implications for the magnetic properties.

Fig.2 compares the unit cell constant and the ionic radii for all of the known $\text{R}_2\text{Mn}_2\text{O}_7$ pyrochlores. The result for $\text{R} = \text{Sc}$ correlates linearly with the values for the phases where $\text{R} = \text{lanthanide}$ or Y and the values for $\text{R} = \text{In}$ and Tl deviate positively from the correlation as noted previously [5]. Such behavior is not unprecedented. Similar deviations have been noted recently for example for the perovskites RCrO_3 , $\text{R} = \text{In}$ and the lanthanides and for the LuMnO_3 structure materials, RMnO_3 , where $\text{R} = \text{In}$, Dy-Sc [11]. The latter case is instructive for the members $\text{R} = \text{Sc}$, In and Lu . In this structure type the Mn-O polyhedron is five coordinate trigonal bipyramidal and the R-O polyhedron is a seven coordinate mono-capped octahedron. While the Mn-O distances scale linearly with the R-radius and differ by no more than 0.01 Å, the anomalously large unit cell volume for $\text{R} = \text{In}$ can be traced to one unusually long In-O bond, the seventh capping oxygen. This was rationalized as a manifestation of the lesser oxygen affinity of d^{10} ions relative to d^0 ions of similar radii. The same principle may be operative in the pyrochlore series. According to Shannon, Tl^{3+} and Yb^{3+} have essentially the same radius in VIII coordination [12]. The Mn-O distances are indeed the same, 1.903(1) Å for Yb and 1.902(2) Å for Tl , but the Tl-O distances are systematically longer, 2.449(1) Å and 2.139(1) Å relative to Yb-O distances 2.423(2) Å and 2.129(1) Å [6,8]. Thus, there may be no need to invoke any significant mixed valency in $\text{Tl}_2\text{Mn}_2\text{O}_7$ to explain the observed bond distances. This issue remains to be settled, probably by spectroscopic investigations.

b.) Magnetic Properties

Figure 3 shows the inverse susceptibility of $\text{Sc}_2\text{Mn}_2\text{O}_7$

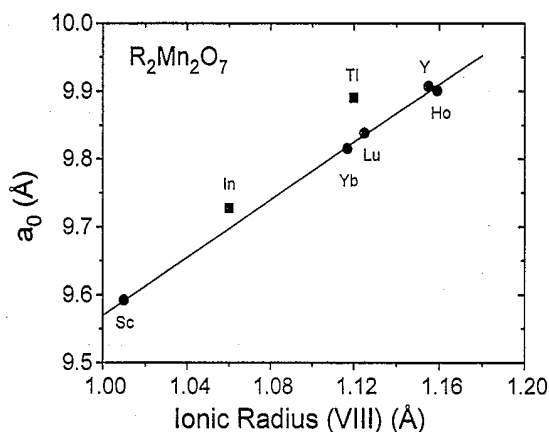


Fig. 2: Lattice constants of $\text{R}_2\text{Mn}_2\text{O}_7$ against radius of R^{3+} .

over the range 5 K to 300 K and including results for $\text{Lu}_2\text{Mn}_2\text{O}_7$ for comparison. Parameters derived from a fit to the Curie-Weiss law, $\chi = C/(T - \theta)$, in the range 200 - 300 K, are $C = 3.17(3)$ emu-K/mol and $\theta = 77(3)$ K. The Curie constant, C , is close to the expected value for $S = 3/2$, 3.75 emu-K/mol for two Mn^{4+} per formula unit. The smaller observed value reflects the presence of 2.3 wt% or 5.1 mol% of diamagnetic Sc_2O_3 .

The θ value is large and positive as found for all members of the $\text{R}_2\text{Mn}_2\text{O}_7$ series, which indicates the dominance of ferromagnetic exchange interactions. Furthermore, the value for $\text{R} = \text{Sc}$ of 77 K is intermediate between those for the spin glass materials, $\text{R} = \text{Y}$ (41 K) and $\text{R} = \text{Lu}$ (46 K) and the ferromagnets $\text{R} = \text{Tl}$ (155 K) and $\text{R} = \text{In}$ (150 K).

Fig.4 shows the d.c. susceptibility at low temperatures and clear field-cooled, zero-field-cooled irreversibility sets in below 17 K which is the same behavior as for $\text{Y}_2\text{Mn}_2\text{O}_7$ and $\text{Lu}_2\text{Mn}_2\text{O}_7$ and is in sharp contrast to that for $\text{In}_2\text{Mn}_2\text{O}_7$

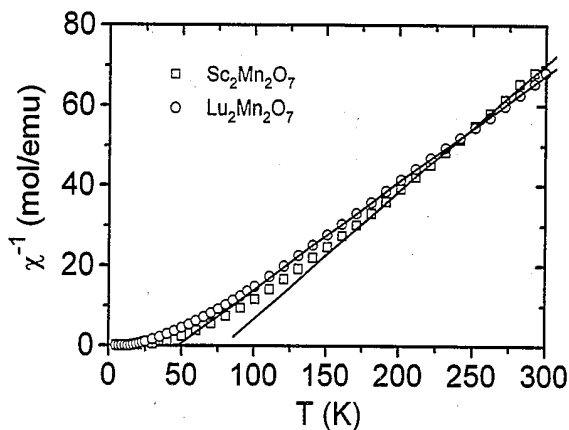


Fig. 3: Inverse molar susceptibilities against temperature for $\text{Sc}_2\text{Mn}_2\text{O}_7$ and $\text{Lu}_2\text{Mn}_2\text{O}_7$.

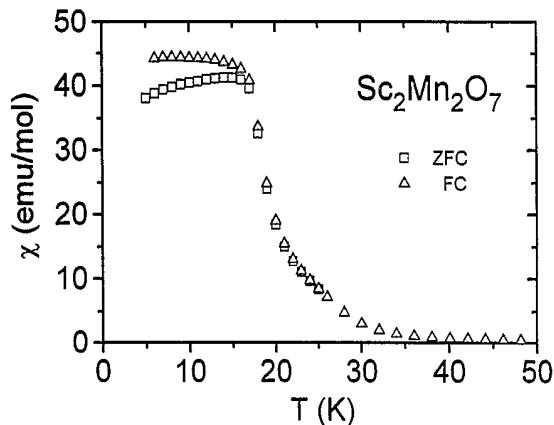


Fig. 4: Zero field cooled (ZFC) and field cooled (FC) susceptibilities for $\text{Sc}_2\text{Mn}_2\text{O}_7$.

and $\text{Tl}_2\text{Mn}_2\text{O}_7$ [4,5]. These results are in rough agreement with previous work but in that work ZFC-FC comparisons were not made [2].

Isothermal magnetization studies at 5 K on $\text{Sc}_2\text{Mn}_2\text{O}_7$ and $\text{Lu}_2\text{Mn}_2\text{O}_7$, Fig.5, indicate a more facile approach to saturation for the former.

In summary the magnetic properties of $\text{Sc}_2\text{Mn}_2\text{O}_7$, particularly the larger, positive θ and the facile saturation indicate enhanced ferromagnetic interactions relative to $\text{Y}_2\text{Mn}_2\text{O}_7$ and $\text{Lu}_2\text{Mn}_2\text{O}_7$. Yet, $\text{Sc}_2\text{Mn}_2\text{O}_7$ remains spin glass like rather than achieving true ferromagnetic order as seen in $\text{Tl}_2\text{Mn}_2\text{O}_7$ and $\text{In}_2\text{Mn}_2\text{O}_7$. There appears to be a correlation, then, between the transport and magnetic properties in this series of compounds. The spin glass phases are either insulating ($R=\text{Sc}$) or semiconducting with high room temperature resistivities, $10^5 - 10^8 \Omega\text{-cm}$, and large activation energies ($R=\text{Y,Lu}$) and the magnetic transition occurs at comparatively low temperatures, 17 K.

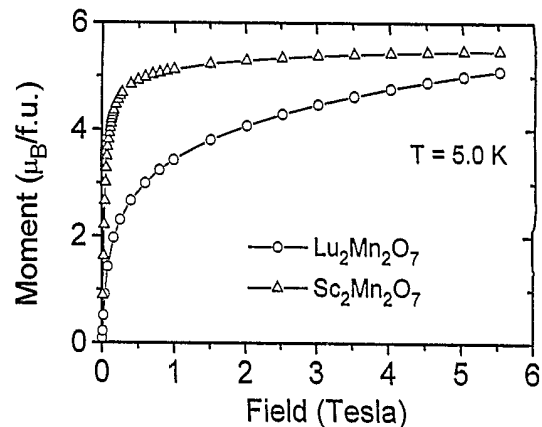


Fig. 5: Magnetization as a function of applied field for $\text{Sc}_2\text{Mn}_2\text{O}_7$ and $\text{Lu}_2\text{Mn}_2\text{O}_7$ at 5 K.

The ferromagnets ($R=\text{Tl,In}$) with $T_c = 120$ K are much better conductors with room temperature resistivities smaller by factors of $10^4 - 10^8$. This is strong evidence that the development of ferromagnetism and possibly GMR effects are directly tied to an enhanced carrier density. Hall effect data for $\text{Tl}_2\text{Mn}_2\text{O}_7$ indicate a very small carrier density, of 1 to 5×10^{-3} electrons per formula unit, relative to other GMR materials [7]. The full relationship between carrier concentration, ferromagnetism and GMR has yet to be established.

Acknowledgements

We acknowledge the financial support of the Natural Science and Engineering Research Council of Canada. We thank Prof. C. V. Stager for use of the SQUID magnetometer and Mr. W. H. Gong for collecting x-ray powder diffraction data.

References

1. H. Fujinaka, N. Kinamura, M. Koizumi, Y. Miyamoto and S. Kume, *Mat. Res. Bull.* **14**, 1133 (1979).
2. I. O. Troyanchuk and V. N. Derachenko, *Sov. Phys. Solid State* **30**, 2003 (1988).
3. M. A. Subramanian, C. C. Torardi, D. C. Johnson, J. Pannetier and A. W. Sleight, *J. Sol. State Chem.* **72**, 24 (1988).
4. J. N. Reimers, J. E. Greedan, R. K. Kremer, E. Gmelin and M. A. Subramanian, *Phys. Rev. B* **43**, 3387 (1991).
5. N. P. Raju, J. E. Greedan and M. A. Subramanian, *Phys. Rev. B* **49**, 1086 (1994).
6. J. E. Greedan, N. P. Raju, A. Maignan, Ch. Simon, J. S. Pedersen, A. M. Niraimathi, E. Gmelin and M. A. Subramanian, submitted to *Phys. Rev. B*
7. Y. Shimakawa, Y. Kubo and T. Manako, *Nature* **379**, 53 (1996); S-W. Cheong, H. Y. Hwang, B. Batlogg and L. W. Rupp Jr., *Solid State Commn.* **98**, (163) (1996).
8. M. A. Subramanian, B. H. Toby, A. P. Ramirez, W. H. Marshall, A. W. Sleight and G. H. Kwei, submitted to *Science*.
9. R. Sakhivel and R. Young, "User's Guide to Programs DBWS-9006 and DBWS-9006PC," 1991. D. B. Wiles and R. Young, *J. Appl. Cryst.* **14**, 149 (1981).
10. R. J. Hill and C. J. Howard, *J. Appl. Cryst.* **20**, 467 (1987).
11. J. E. Greedan, M. Bieringer, J. F. Britten, D. M. Giaquinta and H.-C. zur Loye, *J. Solid State Chem.* **116**, 118 (1995).
12. R. D. Shannon, *Acta. Cryst.* **A32**, 751 (1976).